

Synthesis, Structures, and Reactivity of Nickel Complexes Incorporating Sulfonamido-Imine Ligands

Jianfeng Li, Dawei Tian, Haibin Song, Chunhua Wang, Xiaoqing Zhu, Chunming Cui,* and Jin-Pei Cheng*

State Key Laboratory of Elemento-Organic Chemistry, Nankai University, Tianjin 300071, People's Republic of China

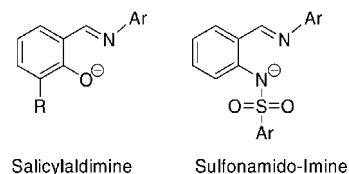
Received January 1, 2008

Nickel complexes incorporating sulfonamido-imine ligands $[o\text{-C(H)NDipp-C}_6\text{H}_4\text{NSO}_2(\text{Ar})]^-$ (Dipp = 2,6-*i*Pr₂C₆H₃; L¹ where Ar = 2,4,6-Me₃C₆H₂, L² where Ar = 4-MeC₆H₄, L³ where Ar = 4-O₂NC₆H₄) were synthesized and characterized. Reaction of L¹Li with *trans*-[Ni(Cl)(Ph)(PPh₃)₂], NiBr₂(THF)_{1.5}, and NiCl₂(Py)₄ resulted in the formation of the nickel(I) complex L¹Ni(PPh₃) (**1**) and the four-coordinate nickel halides L¹Ni(Br)(THF) (**2**) and L¹Ni(Cl)(Py) (**3**), respectively. In contrast, reactions of less hindered L²Li and L³Li with NiBr₂(DME) yielded the bis(sulfonamido-imine)nickel complexes (L²)₂Ni (**4**) and (L³)₂Ni (**5**). Alkylation of **2** with LiCH₂SiMe₃ afforded the neutral nickel alkyl L¹Ni(CH₂SiMe₃) (**6**). The molecular structures of **1–5** have been determined by X-ray single-crystal analysis. DFT calculations revealed that **6** adopts a distorted square-planar geometry with one of the oxygen atoms of the sulfonyl group being bound to the nickel center.

Introduction

In recent years, there has been great interest in the synthesis and characterization of single-site polymerization catalysts based on nickel, palladium, and other late transition metals.¹ These metal complexes are less electrophilic and, therefore, tolerant to a wide range of organic functional groups. Pioneer work by Brookhart and Grubbs has shown that cationic nickel and palladium alkyls incorporating α -diimine ligands² and neutral salicylaldimine nickel complexes³ are viable for the copolymerization of ethylene and polar monomers. Since then, a number of different types of monoanionic bidentate ligands with N, P, and O donors have been employed for this purpose.⁴ These studies indicate that suitable ligand frameworks could result in highly efficient copolymerization catalysts. In this vein, we are interested in developing alternative ligand systems to support nickel alkyls and explore their structures and reactivity.

Chart 1



We have previously reported the coordination chemistry of monoanionic sulfonamido aluminum complexes.⁵ We now extend this ligand family to mimic well-known salicylaldimine ligand sets considering that the acidity of sulfonamides is similar to that of phenols as a result of the electron-withdrawing nature of the sulfonyl group (Chart 1). In addition, one of the oxygen atoms on a sulfonyl group may have, to some extent, interaction with the central metal atom, resulting in a unique coordination environment and modification of reactivity of the corresponding metal complexes. It is anticipated that the oxygen atoms of a sulfonyl group may act as a potential hamilabile arm due to the relatively weak coordination ability of the oxygen atom to late transition metals. It has been shown that the low-coordinate and electronically unsaturated active metal center can be stabilized by hemilabile arms, which are capable of reversible dissociation from the metal center to provide a vacant coordination site for bonding of incoming substrates.⁶ Herein we report on the synthesis and structures of novel nickel complexes bearing sulfonamido-imine ligands.

Experimental Section

All manipulations involving air- and moisture-sensitive compounds were carried out under an atmosphere of dry argon by using modified Schlenk line and glovebox techniques. Elemental analyses

* Corresponding author. E-mail: cmcui@nankai.edu.cn.

(1) Reviews: (a) Boffa, L. S.; Novak, B. M. *Chem. Rev.* **2000**, *100*, 1479. (b) Mecking, S. *Coord. Chem. Rev.* **2000**, *203*, 325. (c) Ittel, S. D.; Johnson, L. K.; Brookhart, M. *Chem. Rev.* **2000**, *100*, 1169. (d) Gibson, V. C.; Spitzmesser, S. K. *Chem. Rev.* **2003**, *103*, 283.

(2) (a) Johnson, L. K.; Mecking, S.; Brookhart, M. *J. Am. Chem. Soc.* **1996**, *118*, 267. (b) Mecking, S.; Johnson, L. K.; Wang, L.; Brookhart, M. *J. Am. Chem. Soc.* **1998**, *120*, 888.

(3) Younkin, T. R.; Connor, E. F.; Henderson, J. I.; Friedricj, S. K.; Grubbs, R. H.; Bansleben, D. A. *Science* **2000**, *287*, 460.

(4) (a) Gibson, V. C.; Tomov, A. *Chem. Commun.* **2001**, 1964. (b) Soula, R.; Saillard, B.; Spitz, R.; Claverie, J.; Llauro, M. F.; Monnet, C. *Macromolecules* **2002**, *35*, 1513. (c) Drent, E.; Dijk, R. V.; Ginkel, R. V.; Oort, B. V.; Pugh, R. I. *Chem. Commun.* **2002**, 744. (d) Britovsek, G. J. P.; Gibson, V. C.; Spitzmesser, S. K.; Tellman, K. P.; White, A. J. P.; Williams, D. J. *J. Chem. Soc., Dalton Trans.* **2002**, 1159. (e) Li, X.-F.; Li, Y.-G.; Li, Y.-S.; Chen, Y.-X.; Hu, N.-H. *Organometallics* **2005**, *24*, 2502. (f) Groux, L. F.; Weiss, T.; Reddy, D. N.; Chase, P. A.; Piers, W. E. *J. Am. Chem. Soc.* **2005**, *127*, 1854. (g) Carlini, C.; De Luise, V.; Martinelli, M.; Galletti, A. M. R.; Sbrana, G. *J. Polym. Sci., Part A: Polym. Chem.* **2006**, *44*, 620. (h) Galletti, A. M. R.; Carlini, C.; Giaiacopi, S.; Martinelli, M.; Sbrana, G. *J. Polym. Sci., Part A: Polym. Chem.* **2007**, *45*, 1134. (i) Carone, C. L. P.; Bisatto, R.; Galland, G. B.; Rojas, R.; Bazan, G. *J. Polym. Sci., Part A: Polym. Chem.* **2008**, *46*, 54.

(5) Zhao, J.; Song, H.; Cui, C. *Organometallics* **2007**, *26*, 1947.

(6) For examples, see: (a) Dove, A. P.; Gibson, V. C.; Marshall, E. L.; White, A. J. P.; Williams, D. J. *Dalton Trans.* **2004**, 570. (b) Wang, X.; Liu, S.; Jin, G.-X. *Organometallics* **2004**, *23*, 6002.

were carried out on an Elemental Vario EL analyzer. The ^1H and ^{13}C NMR spectroscopic data were recorded on a Varian Mercury Plus 400 spectrometer. Infrared spectra were recorded on a Bio-Rad FTS 6000 spectrophotometer. The solvents (THF, toluene, *n*-hexane, and diethyl ether) were freshly distilled from sodium and degassed prior to use. Methylene chloride was dried over CaH_2 and freshly distilled and degassed prior to use. The free ligand precursors *o*-CHO-C₆H₄NHSO₂(Ar) (Ar = 2,4,6-Me₃C₆H₂, 4-MeC₆H₄, 4-O₂NC₆H₄)⁷ and the nickel halides NiBr₂(THF)_{1.5},⁸ NiBr₂(DME),⁹ NiCl₂(Py)₄,¹⁰ *trans*-[Ni(Cl)(Ph)(PPh₃)₂],¹¹ and LiCH₂SiMe₃¹² were synthesized according to the published procedures.

Synthesis of L¹H. A solution of *o*-CHO-C₆H₄NHSO₂(Ar) (Ar = 2,4,6-Me₃C₆H₂) (9.10 g, 30 mmol), 2,6-diisopropylaniline (5.66 mL, 30 mmol), and *p*-toluenesulfonic acid (0.10 g) was refluxed in toluene (160 mL) for 4 h while the resulting water was removed as an azeotrope with a Dean and Stark apparatus. After evaporation, the resulting residue was taken up in CH₂Cl₂ and the extract was washed with saturated aqueous Na₂CO₃. The organic phase was separated, dried over Na₂SO₄, and filtered. L¹H was crystallized from CH₂Cl₂/EtOH (1:5) to give white crystals (12.67 g, 91.4%). Mp: 160 °C. Anal. Calcd for C₂₈H₃₄N₂O₂S (462.23): C, 72.69; H, 7.41; N, 6.06. Found: C, 72.83; H, 7.43; N, 6.39. ^1H NMR (CDCl₃): δ 1.19 (d, $J = 6.86$ Hz, 12H, CHMe₂), 2.28 (s, 3H, *p*-ArMe), 2.73 (s, 6H, *o*-ArMe), 3.03 (sept, $J = 6.86$ Hz, 2H, CHMe₂), 6.95 (s, 2H, Ar H), 7.01–7.20 (m, 7H, Ar H), 8.25 (s, 1H, CH = N), 12.77 (s, 1H, NH). ^{13}C NMR (CDCl₃): δ 20.94 (*p*-ArMe), 22.76 (*o*-ArMe), 23.74 (CHMe₂), 28.11 (CHMe₂), 109.75, 115.72, 119.17, 121.43, 123.27, 125.3, 132.11, 132.28, 134.37, 138.40, 139.32, 139.88, 142.56, 147.10 (Ar C), 165.83 (CH=N). IR (cm⁻¹): $\nu(\text{C}=\text{N})$ 1623, $\nu_{\text{as}}(\text{SO}_2)$ 1336, $\nu_{\text{s}}(\text{SO}_2)$ 1156.

Synthesis of L²H. This compound was prepared from *o*-CHO-C₆H₄NHSO₂(Ar) (Ar = 4-MeC₆H₄) (8.26 g, 30 mmol), 2,6-diisopropylaniline (5.66 mL, 30 mmol), and *p*-toluenesulfonic acid (0.10 g) as described for L¹H. The product was obtained as pale yellow crystals (7.59 g, 58.3%). Mp: 162–163 °C. Anal. Calcd for C₂₆H₃₀N₂O₂S (434.2): C, 71.86; H, 6.96; N, 6.45. Found: C, 71.99; H, 7.09; N, 6.42. ^1H NMR (CDCl₃): δ 1.12 (d, $J = 6.87$ Hz, 12H, CHMe₂), 2.31 (s, 3H, *p*-ArMe), 2.85 (sept, $J = 6.87$ Hz, 2H, CHMe₂), 7.00–7.74 (m, 11H, Ar H), 8.15 (s, 1H, CH=N), 12.62 (s, 1H, NH). ^{13}C NMR (CDCl₃): δ 21.29 (*p*-ArMe), 23.43 (CHMe₂), 28.03 (CHMe₂), 116.99, 119.87, 122.30, 123.14, 125.26, 126.95, 129.45, 132.28, 134.22, 137.06, 137.97, 139.56, 143.60, 146.91 (Ar C), 165.76 (CH=N). IR (cm⁻¹): $\nu(\text{C}=\text{N})$ 1626, $\nu_{\text{as}}(\text{SO}_2)$ 1345, $\nu_{\text{s}}(\text{SO}_2)$ 1167.

Synthesis of L³H. L³H was prepared from *o*-CHO-C₆H₄NHSO₂(Ar) (Ar = 4-O₂NC₆H₄) (9.18 g, 30 mmol), 2,6-diisopropylaniline (5.66 mL, 30 mmol), and *p*-toluenesulfonic acid (0.10 g) as described for L¹H. The product was obtained as pale yellow crystals (12.71 g, 91.1%). Mp: 140–141 °C. Anal. Calcd for C₂₅H₂₇N₃O₄S (465.17): C, 64.50; H, 5.85; N, 9.03. Found: C, 64.56; H, 5.93; N, 9.08. ^1H NMR (CDCl₃): δ 1.20 (d, $J = 6.86$ Hz, 12H, CHMe₂), 2.87 (sept, $J = 6.86$ Hz, 2H, CHMe₂), 7.14–7.47 (m, 6H, Ar H), 7.81 (d, $J = 8.35$ Hz, 1H, Ar H), 8.10 (d, $J = 8.79$ Hz, 2H, Ar H), 8.23 (s, 1H, CH=N), 8.30 (d, $J = 8.79$ Hz, 2H, Ar H), 13.21 (s, 1H, NH). ^{13}C NMR (CDCl₃): δ 23.83 (CHMe₂), 28.50 (CHMe₂), 117.36, 120.42, 123.52, 123.66, 124.51, 125.95, 128.56,

132.93, 134.80, 138.32, 139.13, 146.03, 146.73, 150.39 (Ar C), 166.19 (CH=N). IR (cm⁻¹): $\nu(\text{C}=\text{N})$ 1623, $\nu_{\text{as}}(\text{SO}_2)$ 1348, $\nu_{\text{s}}(\text{SO}_2)$ 1167.

Preparation of L¹Li, L²Li, and L³Li. *n*-BuLi (1.1 equiv, 1.6 M in *n*-hexane) was slowly added to a solution of L¹H, L²H, or L³H in toluene at –78 °C. The color of the solution turned from pale yellow to yellow upon addition. The mixture was warmed to room temperature and stirred for additional 2 h. All volatile materials were removed under vacuum. The remaining powder was washed with *n*-hexane and dried under vacuum. These lithium salts are insoluble in organic solvents and were used directly.

Synthesis of L¹Ni(PPh₃) (1). A solution of L¹Li (468 mg, 1 mmol) in toluene was slowly added to a solution of *trans*-[Ni(Cl)(Ph)(PPh₃)₂] (696 mg, 1 mmol) in toluene at room temperature and stirred overnight. After filtration through Celite, the dark red filtrate was concentrated (ca. 5 mL) and *n*-hexane (30 mL) was added. The resulting red powder was recrystallized from THF/*n*-hexane (1:2) at –35 °C to give red brown crystals (407 mg, 52.1%). Mp: 217–218 °C. Anal. Calcd for C₄₆H₄₈N₂NiO₂PS (782.62): C, 70.60; H, 6.18; N, 3.58. Found: C, 70.13; H, 6.23; N, 3.65. IR (cm⁻¹): $\nu(\text{C}=\text{N})$ 1610, $\nu_{\text{as}}(\text{SO}_2)$ 1334, $\nu_{\text{s}}(\text{SO}_2)$ 1119.

Synthesis of L¹Ni(Br)(THF) (2). A solution of NiBr₂ (240 mg, 1.1 mmol) in THF (50 mL) was refluxed for about 24 h, and then a solution of L¹Li (468 mg, 1 mmol) in THF was added. After the mixture was refluxed 48 h, the volatiles were removed in vacuum. The yellow brown residue was extracted with CH₂Cl₂. After filtration, all volatiles were removed in vacuum. The remaining solid was recrystallized from THF/*n*-hexane (1:2) at –35 °C to yield yellow brown crystals of **2** (301 mg, 45.0%). Mp: 201 °C dec. Anal. Calcd for C₃₂H₄₁BrN₂NiO₃S (670.14): C, 57.16; H, 6.15; N, 4.17. Found: C, 56.62; H, 6.33; N, 3.65. ^1H NMR (CDCl₃): δ –8.59, 0.88, 1.21, 1.27, 1.29, 3.00, 3.21, 5.31, 6.96, 8.27, 10.09, 11.05, 12.79, 16.38, 22.94. IR (cm⁻¹): $\nu(\text{C}=\text{N})$ 1612, $\nu_{\text{as}}(\text{SO}_2)$ 1334, $\nu_{\text{s}}(\text{SO}_2)$ 1117.

Synthesis of L¹Ni(Cl)(Py) (3). A mixture of NiCl₂(Py)₄ (245 mg, 0.55 mmol) and L¹Li (234 mg, 0.5 mmol) in THF (40 mL) was refluxed for 24 h, and then the volatiles were removed in vacuum. The yellow residue was extracted with toluene, and the orange filtrate was concentrated. Storage overnight at –35 °C gave orange crystals of **3** (168 mg, 53.0%). Mp: 210 °C dec. Anal. Calcd for C₃₃H₃₈ClN₅NiO₂S (633.17): C, 62.43; H, 6.03; N, 6.62. Found: C, 62.89; H, 6.17; N, 6.59. ^1H NMR (C₆D₆): δ –7.22, –4.70, 1.42, 1.97, 2.57, 4.64, 9.02, 10.50, 13.52, 17.20, 19.50, 24.01, 48.43. IR (cm⁻¹): $\nu(\text{C}=\text{N})$ 1606, $\nu_{\text{as}}(\text{SO}_2)$ 1305, $\nu_{\text{s}}(\text{SO}_2)$ 1116.

Synthesis of (L²)₂Ni (4). A mixture of NiBr₂(DME) (155 mg, 0.5 mmol) and L²Li (440 mg, 1 mmol) in THF (40 mL) was refluxed for 24 h, and then the volatiles were removed in vacuum. The yellow residue was extracted with CH₂Cl₂, and the yellow solution was filtered. All volatile materials were removed in vacuum. Crystallization from THF at –35 °C yielded orange crystals of **4** (373 mg, 80.9%). Mp: >300 °C. Anal. Calcd for C₅₂H₅₈N₄NiO₄S₂ (924.33): C, 67.46; H, 6.31; N, 6.05. Found: C, 66.95; H, 6.14; N, 6.05. ^1H NMR (C₆D₆): δ –3.77, –2.38, –1.97, 0.82, 1.41, 1.66, 3.58, 5.64, 7.92, 10.38, 16.69, 17.30, 26.70. IR (cm⁻¹): $\nu(\text{C}=\text{N})$ 1603, $\nu_{\text{as}}(\text{SO}_2)$ 1308, $\nu_{\text{s}}(\text{SO}_2)$ 1129.

Synthesis of (L³)₂Ni (5). A mixture of NiBr₂(DME) (155 mg, 0.5 mmol) and L³Li (471 mg, 1 mmol) in THF (40 mL) was refluxed for 24 h, and then the volatiles were removed in vacuum. The yellow residue was extracted with CH₂Cl₂, and the mixture was filtered. All volatiles were removed in vacuum. Crystallization from THF at –35 °C gave yellow crystals of **5** (353 mg, 71.6%). Mp: >300 °C. Anal. Calcd for C₅₀H₅₂N₆NiO₈S₂ (986.26): C, 60.79; H, 5.31; N, 8.51. Found: C, 60.31; H, 5.34; N, 7.71. ^1H NMR (C₆D₆): δ –4.00, –2.61, –2.44, –0.70, 0.29, 0.51, 1.10, 1.57, 8.76, 10.38, 16.78, 17.66, 25.75. IR (cm⁻¹): $\nu(\text{C}=\text{N})$ 1606, $\nu_{\text{as}}(\text{SO}_2)$ 1348, $\nu_{\text{s}}(\text{SO}_2)$ 1140.

(7) Fonseca, M. H.; Eibler, E.; Zabel, M.; König, B. *Tetrahedron: Asymmetry* **2003**, *14*, 1989.

(8) Eckert, N. A.; Bones, E. M.; Lachicotte, R. J.; Holland, P. L. *Inorg. Chem.* **2003**, *42*, 1720.

(9) Huang, S. B. Masteral Dissertation, University of Zhejiang, 2006.

(10) Kenessey, G.; Liptay, G. *J. Therm. Anal.* **1993**, *39*, 333.

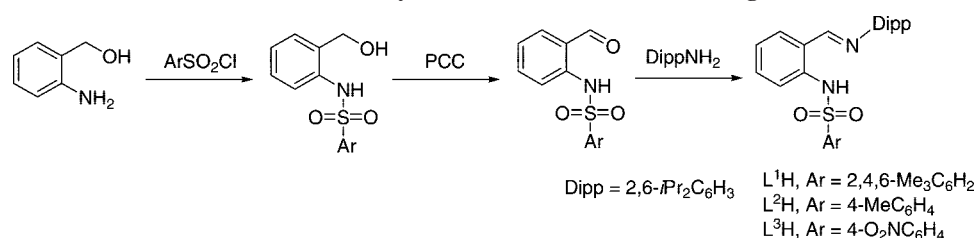
(11) Zeller, A.; Herdtweck, E.; Strassner, T. *Eur. J. Inorg. Chem.* **2003**, 1802.

(12) Vaughn, G. D.; Krein, K. A.; Gladysz, J. A. *Organometallics* **1986**, *5*, 936.

Table 1. Crystallographic Detail for 1–5

	1	2	3 · 3/2C ₇ H ₈	4 · 6C ₄ H ₈ O	5 · 4C ₄ H ₈ O
formula	C ₄₆ H ₄₈ N ₂ NiO ₂ PS	C ₃₂ H ₄₁ BrN ₂ NiO ₃ S	C _{43.5} H ₅₀ ClN ₃ NiO ₂ S	C ₇₆ H ₁₀₆ N ₄ NiO ₁₀ S ₂	C ₆₆ H ₈₄ N ₆ NiO ₁₂ S ₂
fw	782.60	672.35	773.09	1358.48	1276.22
T (K)	294(2)	113(2)	113(2)	113(2)	113(2)
space group	P $\bar{1}$	P $\bar{1}$	C2/c	P2 ₁ /n	P2/c
a (Å)	9.381(6)	8.277(4)	51.72(2)	12.7320(7)	14.6947(19)
b (Å)	10.605(7)	9.648(5)	14.234(6)	15.4904(6)	10.0558(13)
c (Å)	19.553(12)	20.574(11)	11.046(5)	36.9865(18)	22.450(2)
α (deg)	76.759(11)	77.699(11)	90	90	90
β (deg)	88.739(10)	81.838(18)	101.719(5)	98.778(2)	104.286(6)
γ (deg)	83.266(10)	77.803(15)	90	90	90
V (Å ³)	1881(2)	1560.9(14)	7962(6)	7209.2(6)	3214.8(7)
Z	2	2	8	4	2
d _{calcd} (Mg/m ³)	1.382	1.431	1.290	1.252	1.318
F(000)	826	700	3272	2920	1356
GOF	1.028	0.873	1.136	1.063	1.111
R1, wR2 (I > 2σ(I))	0.0864, 0.2186	0.0458, 0.0994	0.0650, 0.1367	0.0877, 0.2368	0.0593, 0.1295
R1, wR2 (all data)	0.1271, 0.2597	0.0680, 0.1089	0.0759, 0.1426	0.1015, 0.2487	0.0680, 0.1345

Scheme 1. General Synthesis of Sulfonamido-Imine Ligands



Synthesis of L¹Ni(CH₂SiMe₃) (6). LiCH₂SiMe₃ (50 mg, 0.53 mmol) in Et₂O was added to **2** (370 mg, 0.55 mmol) in Et₂O at -78 °C. The mixture was warmed to room temperature and stirred continuously for 2 h. All volatile materials were removed under vacuum. The yellow residue was extracted with 10 mL of *n*-hexane, and the red filtrate was concentrated. Storage at -35 °C overnight afforded red brown crystals of **6** (111 mg, 34.7%). Mp: 174–176 °C. Anal. Calcd for C₃₂H₄₄N₂NiO₂SSi (606.22): C, 63.26; H, 7.30; N, 4.61. Found: C, 62.97; H, 7.57; N, 4.32. ¹H NMR (C₆D₆): δ -0.91 (d, ²J_{HH} = 12.02 Hz, 1H, NiCHH), -0.63 (d, ²J_{HH} = 12.03 Hz, 1H, NiCHH), 0.44 (s, 9H, Si(CH₃)₃), 0.86 (d, *J* = 6.73 Hz, 3H, CHMe₂), 1.08 (d, *J* = 6.85 Hz, 3H, CHMe₂), 1.33 (d, *J* = 6.78 Hz, 3H, CHMe₂), 1.62 (d, *J* = 6.83 Hz, 3H, CHMe₂), 1.83 (s, 3H, *p*-ArMe), 3.30 (s, 6H, *o*-ArMe), 3.50 (sept, *J* = 6.66 Hz, 1H, CHMe₂), 4.70 (sept, *J* = 6.93 Hz, 1H, CHMe₂), 6.37–7.02 (m, 9H, Ar H), 7.14 (s, 1H, CH=N). ¹³C NMR (C₆D₆): δ -8.25 (NiCH₂), 2.38 (Si(CH₃)₃), 20.72, 23.02, 23.18, 23.97, 24.70, 24.99, 28.20, 28.82 (CHMe₂, CHMe₂, *p*-ArMe, *o*-ArMe), 117.37, 119.91, 121.87, 123.45, 123.85, 127.27, 132.58, 134.29, 135.40, 135.95, 139.25, 139.44, 140.19, 142.54, 149.91 (Ar C), 167.58 (CH=N). IR (cm⁻¹): ν(C=N) 1603, ν_{as}(SO₂) 1290, ν_s(SO₂) 1105.

Ethylene Polymerization. Ethylene polymerization was performed in a 100 mL autoclave. After evacuation and flushing with nitrogen three times, then with ethylene two times, the autoclave was charged with 30 mL of toluene and stirred under ambient ethylene atmosphere. When the ethylene pressure was raised to 10 atm and temperature was kept at 40 °C, 7 μmol Ni complex and 1.2 mL of MAO (10% in toluene, Al:Ni 260:1) were injected into the reactor. After 30 min it was quickly cooled down to 20 °C, and then quenched by adding ethanol/HCl (10%) to give polyethylene.

Computational Methods. The DFT calculations were carried out with Gaussian 03.¹³ The density functional hybrid model B3LYP was used together with the basis set 6-31g for C, S, O, Br, Si, N, H and Lanl2dz for Ni.

X-ray Structural Determination. All intensity data were collected with a Bruker SMART CCD diffractometer, using graphite-

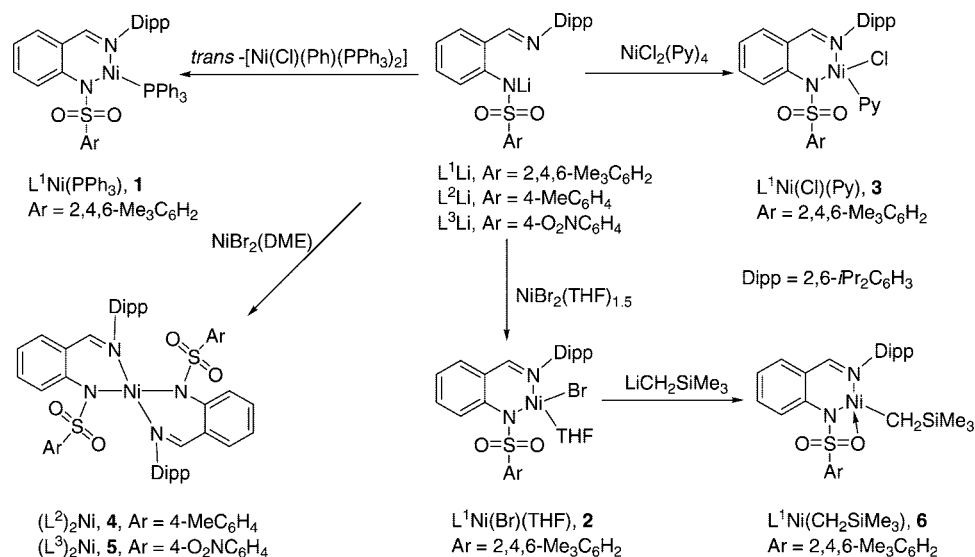
monochromated Mo Kα radiation (λ = 0.71073 Å). The structures were resolved by direct methods and refined by full-matrix least-squares on *F*². Hydrogen atoms were considered in calculated positions. All non-hydrogen atoms were refined anisotropically. Crystal data and data collection details are collected in Table 1. Crystals of **1**, **2**, and **5** suitable for X-ray analysis were obtained from THF/*n*-hexane at room temperature, **3** was obtained from toluene at room temperature, and **4** was obtained from THF at -35 °C.

Results and Discussion

Synthesis of Ligands. The ligands were synthesized by standard condensation reactions of the corresponding aldehydes⁷ and anilines (Scheme 1). By selection of easily available arylsulfonyl chlorides and anilines, the steric and electronic properties of the ligands can be tuned. Thus, they are potential spectator ligands for metal complexes. All of these ligands have been characterized by elemental analyses and ¹H NMR, ¹³C NMR, and IR spectroscopy. Deprotonation of these free ligands was accomplished with *n*-BuLi in toluene to afford pale yellow powders (L¹Li, L²Li, and L³Li). These lithium salts can be used directly without further purification.

(13) Frisch, M. J.; Trucks, G. W.; Schlegel, H. B.; Scuseria, G. E.; Robb, M. A.; Cheeseman, J. R.; Montgomery, J. A., Jr.; Vreven, T.; Kudin, K. N.; Burant, J. C.; Millam, J. M.; Iyengar, S. S.; Tomasi, J.; Barone, V.; Mennucci, B.; Cossi, M.; Scalmani, G.; Rega, N.; Petersson, G. A.; Nakatsuji, H.; Hada, M.; Ehara, M.; Toyota, K.; Fukuda, R.; Hasegawa, J.; Ishida, M.; Nakajima, T.; Honda, Y.; Kitao, O.; Nakai, H.; Klene, M.; Li, X.; Knox, J. E.; Hratchian, H. P.; Cross, J. B.; Bakken, V.; Adamo, C.; Jaramillo, J.; Gomperts, R.; Stratmann, R. E.; Yazyev, O.; Austin, A. J.; Cammi, R.; Pomelli, C.; Ochterski, J. W.; Ayala, P. Y.; Morokuma, K.; Voth, G. A.; Salvador, P.; Dannenberg, J. J.; Zakrzewski, V. G.; Dapprich, S.; Daniels, A. D.; Strain, M. C.; Farkas, O.; Malick, D. K.; Rabuck, A. D.; Raghavachari, K.; Foresman, J. B.; Ortiz, J. V.; Cui, Q.; Baboul, A. G.; Clifford, S.; Cioslowski, J.; Stefanov, B. B.; Liu, G.; Liashenko, A.; Piskorz, P.; Komaromi, I.; Martin, R. L.; Fox, D. J.; Keith, T.; Al-Laham, M. A.; Peng, C. Y.; Nanayakkara, A.; Challacombe, M.; Gill, P. M. W.; Johnson, B.; Chen, W.; Wong, M. W.; Gonzalez, C.; Pople, J. A. *Gaussian 03*, revision C.01; Gaussian, Inc.: Wallingford, CT, 2004.

Scheme 2. Synthesis of Nickel Complexes



Synthesis of Nickel Complexes 1–5. The nickel complexes **1–5** shown in Scheme 2 were synthesized by reactions of appropriate nickel halides with the lithium salts L^1Li , L^2Li , and L^3Li . Reaction of the bulky L^1Li with *trans*-[Ni(Cl)(Ph)(PPh₃)₂] in toluene yielded the three-coordinate nickel(I) complex $L^1Ni(PPh_3)$ (**1**) as red brown crystals. Similar Ni(I) complexes have been generated by the reaction of *trans*-[Ni(Cl)(Ph)(PPh₃)₂] with an imido-imine and bulky β -diketiminato lithium salts.^{14,15} However, reactions of L^2Li and L^3Li with *trans*-[Ni(Cl)(Ph)(PPh₃)₂] yielded a complicated mixture, which cannot be either separated or identified definitely. For the synthesis of divalent nickel alkyls, nickel halides might be good precursors. Thus, reaction of L^1Li with NiBr₂(THF)_{1.5} or NiCl₂(Py)₄ in refluxing THF afforded the four-coordinate nickel halides **2** as yellow brown crystals and **3** as orange crystals, respectively. However, reactions of the less hindered lithium salts L^2Li and L^3Li with NiBr₂(DME) in refluxing THF yielded the bis(sulfonamido-imine) nickel complexes **4** (orange crystals) and **5** (yellow crystals), irrespective of the molar ratio of the lithium salts and NiBr₂(DME) employed. The formation of **4** and **5** apparently resulted from the less hindered aryl groups on the sulfonyl group. It is surprising that L^2Li and L^3Li do not react with NiCl₂(Py)₄ under the same conditions as for the synthesis of **3–5**, probably due to the lower reactivity of NiCl₂(Py)₄ than NiBr₂(DME). All these paramagnetic complexes **1–5** have been characterized by elemental analyses and ¹H NMR and IR spectroscopy. The IR spectra of these complexes show stretching vibration bands of C=N at 1603–1612 cm⁻¹, which are red-shifted compared to those of the corresponding free ligands (1623–1626 cm⁻¹). The molecular structures of **1–5** were determined by X-ray single-crystal analysis. The X-ray crystallographic data for **1–5** are summarized in Table 1. The structures are shown in Figures 1–5 with the relevant bond parameters.

Crystal Structures of Nickel Complexes 1–5. The structure of **1** in Figure 1 shows that the nickel atom is three-coordinate, being bound to the sulfonamido-imine ligand in an η^2 fashion and one triphenylphosphine ligand. The geometry of the nickel atom can be best described as distorted trigonal-planar (the sum of the three angles around the nickel center = 360°). The very close Ni1–O1 (2.495 Å) distance indicates the existence of a

nonbonding interaction between the two atoms, resulting in the lengthening of the S1–O1 bond (S1–O1 = 1.412(5) Å compared to S1–O2 = 1.391(5) Å). Consequently, the N2–Ni–P1 angle of 148.27(17)° is much more open in comparison to the N1–Ni–P1 of 119.15(18)°. The Ni–N and Ni–P bond lengths are only slightly shorter than those observed in the previously reported three-coordinate nickel(I) complexes shown in Table 2. The short C–N bond length of 1.262(8) Å reveals an essentially double bond character, indicating little electron delocalization through the imine system.

The molecular structures of **2** and **3** are shown in Figures 2 and 3, respectively. The two nickel halides feature a distorted tetrahedral geometry with almost orthogonal N1–Ni1–N2 angles (90.83(12)° in **2** and 89.55(12)° in **3**). The Ni–N bond lengths of 1.971(3) and 2.029(3) Å in **2** and 1.975(3) and

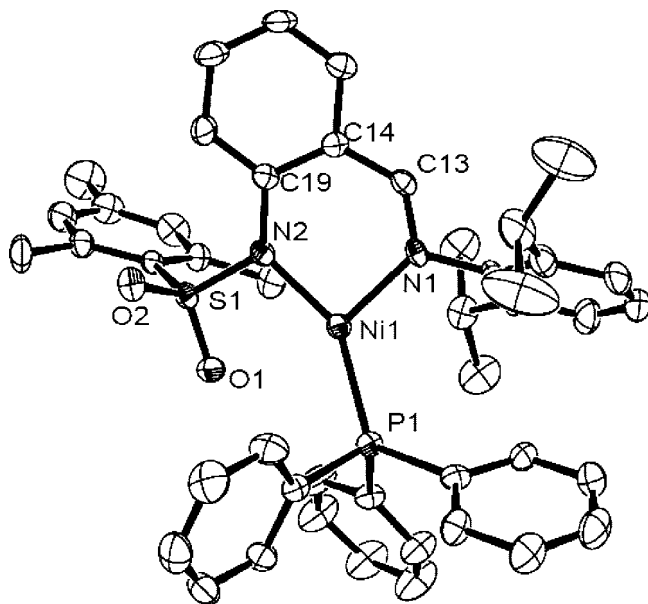


Figure 1. ORTEP representation of the X-ray structure of **1**. Hydrogen atoms have been omitted for clarity. Thermal ellipsoids are drawn at 30% probability. Selected bond lengths (Å) and angles (deg): Ni1–N1 1.906(5), Ni1–N2 1.878(6), Ni1–P1 2.167(2), Ni1–O1 2.495, N1–C13 1.262(8), S1–O1 1.412(5), S1–O2 1.391(5), S1–N2 1.566(5), N1–Ni1–N2 92.3(2), N1–Ni1–P1 119.15(18), N2–Ni1–P1 148.27(17).

(14) Wang, H.-Y.; Meng, X.; Jin, G.-X. *Dalton Trans.* **2006**, 2579.

(15) Zhang, D.; Jin, G.-X.; Weng, L.-H.; Wang, F.-S. *Organometallics* **2004**, *23*, 3270.

Table 2. Comparison of the Relevant Bond Lengths (Å) and Angles (deg) in the Related Three-Coordinate Nickel(I) Complexes^a

	Ni–N	Ni–P	N–Ni–N
[<i>o</i> -C(H)NDipp-C ₆ H ₄ NDipp]Ni(PPh ₃)	1.908(4)–1.970(4)	2.233(2)	94.56(8)
[<i>o</i> -C(H)NAr-C ₆ H ₄ NDipp]-Ni(PPh ₃) ^b	1.899(2)–1.933(2)	2.2096(9)	95.27(8)
{HC[C(Me)NDipp] ₂ }-Ni(PPh ₃)	1.899(3)–1.911(3)	2.2044(12)	96.77(14)
{HC[C(Me)NDipp] ₂ }-Ni(PCy ₃)	1.943(2)–1.957(2)	2.2786(8)	96.70(9)
L ¹ Ni(PPh ₃)	1.878(6)–1.906(5)	2.1167(2)	92.3(2)

^a All data taken from refs 14–16 except those in L¹Ni(PPh₃), Dipp = 2,6-*i*Pr₂C₆H₃. ^b Ar = 2,6-Me₂C₆H₃.

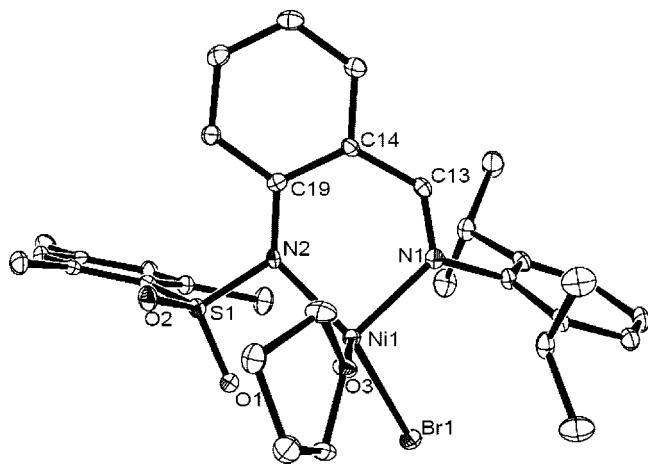


Figure 2. ORTEP representation of the X-ray structure of **2**. Hydrogen atoms have been omitted for clarity. Thermal ellipsoids are drawn at 30% probability. Selected bond lengths (Å) and angles (deg): Ni1–N1 2.029(3), Ni1–N2 1.971(3), Ni1–O1 2.348, Ni1–O3 2.026(2), Ni1–Br1 2.363(1), S1–N2 1.617(3), S1–O1 1.471(2), S1–O2 1.443(2), N1–C13 1.285(4), N2–C19 1.377(4), C13–C14 1.463(5), C14–C19 1.431(5), N1–Ni1–O3 102.50(10), N1–Ni1–Br1 102.16(8), N1–Ni1–N2 90.83(12).

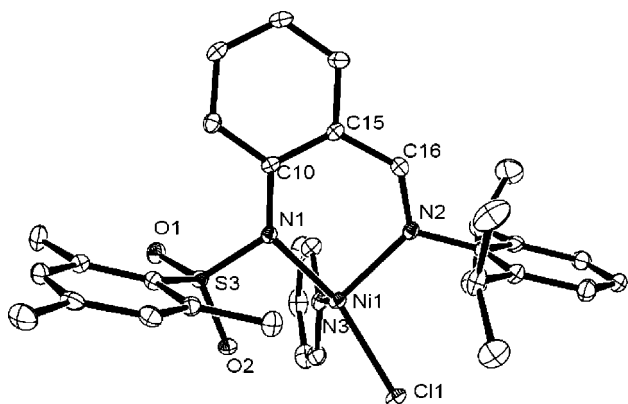


Figure 3. ORTEP representation of the X-ray structure of **3**. Hydrogen atoms have been omitted for clarity. Thermal ellipsoids are drawn at 30% probability. Selected bond lengths (Å) and angles (deg): Ni1–N1 1.975(3), Ni1–N2 2.028(3), Ni1–N3 2.018(3), Ni1–C11 2.246(5), Ni1–O2 2.377, N1–S3 1.621(3), N1–O1 1.378(4), N2–C16 1.294(5), S3–O1 1.438(3), S3–O2 1.463(3), C10–C15 1.415(5), C15–C16 1.448(5), N1–Ni1–N3 101.73(12), N1–Ni1–N2 89.55(12), N2–Ni1–N3 105.87(12), N2–Ni1–C11 101.38(9).

2.028(3) Å in **3** are longer than those in **1** because of the high coordination number of **2** and **3**. The Ni1–Br1 bond length of 2.363(1) Å for **2** falls in the range of 2.352(1) to 2.376(1) Å for

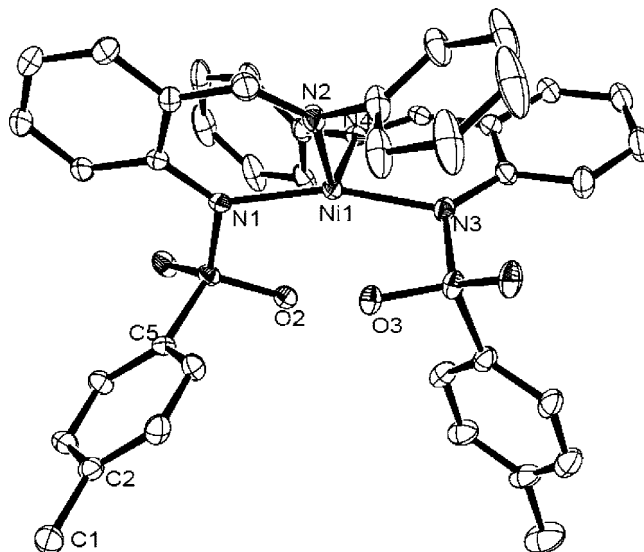


Figure 4. ORTEP representation of the X-ray structure of **4**. Hydrogen atoms and *i*Pr groups have been omitted for clarity. Thermal ellipsoids are drawn at 30% probability. Selected bond lengths (Å) and angles (deg): Ni1–N1 1.995(4), Ni1–N2 2.036(4), Ni1–N3 1.990(4), Ni1–N4 2.049(4), Ni1–O2 2.510, Ni1–O3 2.447, N1–Ni1–N2 88.59(15), N3–Ni1–N4 87.38(15), N1–Ni1–N3 162.50(15), N2–Ni1–N4 115.88(17).

the four-coordinate nickel bromides {[*o*-C(H)NAr-C₆H₄NAr]-Ni(Br)}₂ (Ar = 2,6-Me₂C₆H₃, 2,6-*i*Pr₂C₆H₃)¹⁷ and {HC[C(Me)-NAr]₂}Ni(Br)(PPh₃) (Ar = 2,6-Me₂C₆H₃).¹⁸ The Ni1–C11 bond length of 2.246(5) Å in **3** is slightly shorter than those observed in four-coordinate nickel chlorides [{HC[C(Me)NDipp]₂}Ni(Cl)]₂ (2.324(1)–2.349(1) Å).⁸ The Ni–O(sulfonyl) distances of 2.348 Å in **2** and 2.377 Å in **3** are shorter by ca. 0.15 and 0.12 Å, respectively, than that observed in **1**, but still longer than the sum of the covalent radius of Ni and O (2.18 Å). Consistent with the close Ni–O interaction, the S–O double bond was elongated by 0.028 Å in **2** and 0.025 Å in **3** compared to a normal S–O double bond, and the halide ligands in **2** and **3** are pushed from the bisector of the N1–Ni1–N2 to the imine group.

The molecular structures of **4** and **5** are shown in Figures 4 and 5 with selected bond parameters. In the solid state, **4** is essentially C₂ symmetric and **5** has a crystallographically required C₂ symmetry. Both compounds adopt a distorted tetrahedral geometry. The most striking feature for the bis-ligated complexes is the unusual wide N1–Ni1–N3 (162.50(15)°) angle observed in **4** and N2–Ni1–N2* (163.86(15)°) in **5**. Consequently, the Ni–N(sulfonyl) bond lengths (1.990(4)–2.001(2) Å) in **4** and **5** are slightly longer than those found in **2** and **3** (1.971(3) and 1.975(3) Å). The wide N–Ni–N angle might result from the close contact of the nickel atom with one of the oxygen atoms on the sulfonyl group (2.447–2.647 Å). The Ni–N(imine) bond lengths in **4** and **5** (2.032(3)–2.049(4) Å) are comparable to those in complexes **2** and **3**. The overall geometry of **4** and **5** is quite distinct from that of the bis(anilino-imine) nickel complex [*o*-C(H)N(C₆H₆)-C₆H₄N(C₆H₆)₂Ni],¹⁴ indicating that the close Ni–O interaction has a significant influence on the structure and geometry of metal complexes.

(16) Bai, G.; Wei, P.; Stephan, D. W. *Organometallics* **2005**, *24*, 5901.

(17) Gao, H.; Gao, W.; Bao, F.; Gui, G.; Zhang, J.; Zhu, F.; Wu, Q. *Organometallics* **2004**, *23*, 6273.

(18) Zhang, L.; Ke, Z.; Bao, F.; Long, J.; Gao, H.; Zhu, F.; Wu, Q. *J. Mol. Catal. A* **2006**, *249*, 31.

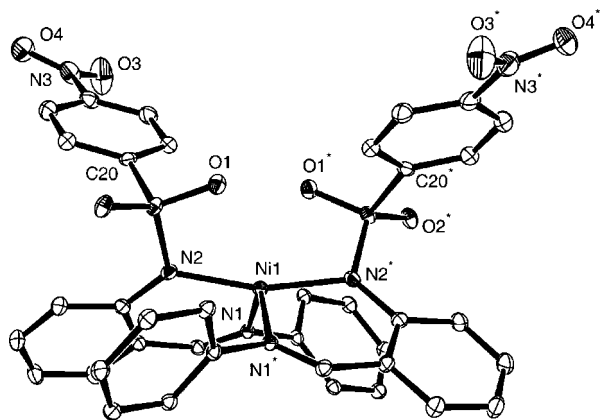


Figure 5. ORTEP representation of the X-ray structure of **5**. Hydrogen atoms and *iPr* groups have been omitted for clarity. Thermal ellipsoids are drawn at 30% probability. Selected bond lengths (Å) and angles (deg): Ni1–N1 2.032(3), Ni1–N2 2.001(2), Ni1–O1 2.647, N1–Ni1–N2 88.74(10), N1–Ni1–N1* 118.40(14), N2–Ni1–N2* 163.86(15).

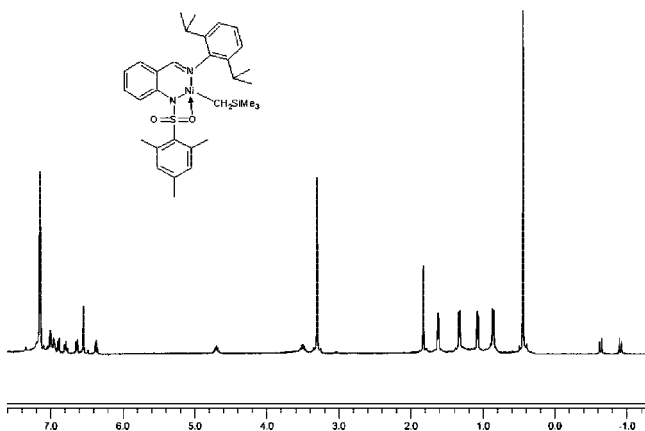


Figure 6. ^1H NMR spectrum of **6** in C_6D_6 at 22 °C.

Alkylation of Nickel Complexes 2 and 3. Attempts to prepare well-defined nickel alkyls by the reactions of halides **2** and **3** with several kinds of lithium alkyls and Grignard reagents have been, so far, unsuccessful. However, reaction of $\text{LiCH}_2\text{-SiMe}_3$ with **2** afforded the desired air- and moisture-sensitive complex **6** as red brown crystals in modest yield (Scheme 2). Compound **6** has been characterized by elemental analysis and ^1H NMR, ^{13}C NMR, and IR spectroscopy. The ^1H NMR spectrum (Figure 6) disclosed that **6** is a solvent-free species. Both the ^1H and ^{13}C NMR spectra of **6** showed a singlet (δ 0.44 and 2.38 ppm, respectively) for the methyl protons and carbons of the CH_2SiMe_3 group, suggesting a small rotation barrier for the SiMe_3 group. The ^1H NMR spectrum shows two doublets (δ –0.91 and –0.63 ppm, $^2J_{\text{HH}} = 12.0$ Hz) for the diastereotopic protons of the methylene group in CH_2SiMe_3 , indicating C_1 symmetry of the molecule. Unfortunately, we were unable to obtain single crystals of **6** suitable for X-ray diffraction studies under various conditions.

The ^1H NMR spectra of **6** in toluene- d_8 from –80 to 50 °C showed similar patterns at these temperatures except that the chemical shift differences of the two doublets for the methylene resonances become smaller with the increase of the temperature (Supporting Information), indicating that the molecular geometry is maintained throughout the temperatures. As compound **6** is decomposed above 50 °C in toluene- d_8 , further information on the structure of **6** at high temperatures could not be obtained

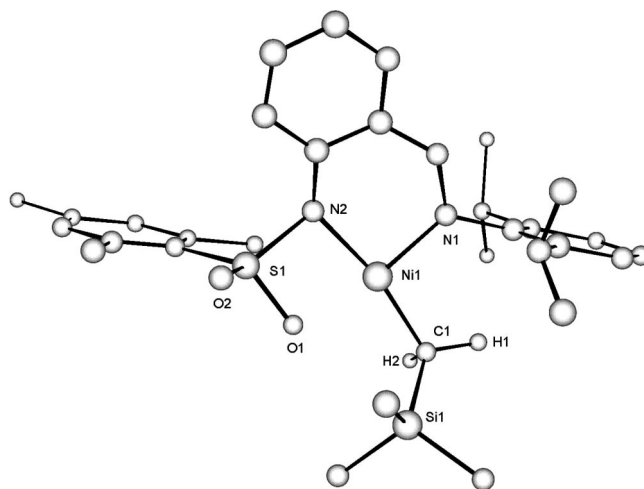


Figure 7. Optimized structure of **6** (DFT; only hydrogen atoms on C1 are shown). Selected bond lengths (Å) and angles (deg): Ni1–C1 1.937, Ni1–N1 1.930, Ni1–N2 1.950, Ni1–O1 2.018, N1–Ni1–N2 91.4, N1–Ni1–C1 99.54.

Table 3. Ethylene Polymerization Results by **1**, **2**, and **6** Combined with MAO^a

entry	complex	yield/g	activity ^b	$10^{-3}M_w^c$	PDI ^c
1	1	0.271	77	97	2.4
2	2	0.088	25	152	2.0
3	6	0.204	58	169	2.1

^a Conditions: 7 μmol of complexes **1**, **2**, and **6**, ethylene pressure = 10 atm, 40 °C, 30 min, 30 mL of toluene, Al/Ni = 260. ^b kg/mol-Ni·h. ^c M_w and PDI (M_w/M_n) were determined by GPC vs polystyrene standards.

from the VT NMR studies. To understand the coordination properties of **6**, DFT calculations with the B3LYP approach were performed (Supporting Information). The optimized structure of **6** (Figure 7) revealed that one of the oxygen atoms on the sulfonyl group is coordinated to the nickel center (Ni–O(sulfonyl) = 2.018 Å). The nickel atom is four-coordinate and adopts a distorted square-planar configuration (the sum of the internal angles = 360°). This geometry is well-correlated with the experimental NMR data in solution. It is noted that four-coordinate nickel alkyl with symmetric pincer-type ligands are known.¹⁹

Ethylene Polymerization. Compounds **1**, **2**, and **6** have been investigated as catalysts for ethylene polymerization reactions. They are active for ethylene polymerization when combined with methylaluminoxane (MAO).²⁰ The polymerization results are summarized in Table 3. All of them showed modest activity. The Ni(II) complexes **2** and **6** gave high molecular weight polyethylene (PE; $M_w \approx 1.5 \times 10^5 - 1.7 \times 10^5$) with narrow polydispersity indices (PDI = 2.0–2.1). In contrast, the Ni(I) complex **1** yielded lower molecular weight PE ($M_w = 9.7 \times 10^4$) with relatively broad molecular weight distribution (PDI = 2.4). Complex **6** was found to be inactive for ethylene polymerization in the absence of any activator in C_6D_6 at temperatures ranging from 22 to 45 °C. This behavior may be attributed to the strong bonding of the oxygen atom to the nickel center and ethylene coordination is prohibited. Further explora-

(19) Liang, L.-C.; Chien, P.-S.; Lin, J.-M.; Huang, M.-H.; Huang, Y.-L.; Liao, J.-H. *Organometallics* **2006**, *25*, 1399.

(20) (a) Feldman, J.; McLain, S. J.; Parthasarathy, A.; Marshall, W. J.; Calabrese, J. C.; Arthur, S. D. *Organometallics* **1994**, *16*, 1514. (b) Zhou, M.-S.; Huang, S.-P.; Weng, L.-H.; Sun, W.-H.; Liu, D.-S. *J. Organomet. Chem.* **2003**, *665*, 237.

tion of the reactivity, especially polymerization reactions with other activators, of these novel complexes is currently in progress.

Conclusion

Sulfonamide-imine ligands have been employed for the synthesis of novel mono- and bis(sulfonamido-imine) nickel complexes. The X-ray structural analyses indicate that there exists a nonbonding interaction between one of the oxygen atoms on the sulfonyl group and nickel center for complexes **1–5** as evidenced by the long S–O distances and short Ni–O contacts. The interaction not only effects the changes in the structural parameters but also favors the formation of the mononuclear halides **2** and **3**. The bulky alkyl ligand CH₂SiMe₃

renders the formation of the solvent-free nickel alkyl **6**, in which the bonding interaction of the Ni–O has been proposed by DFT calculations.

Acknowledgment. This work was supported by the National Natural Science Foundation of China (NSFC), the Key Project of Chinese Ministry of Education, and the 111 Plan.

Supporting Information Available: Computational details for compounds **2** and **6**, VT NMR studies for compound **6**, and CIF files for compounds **1–5**. This material is available free of charge via the Internet at <http://pubs.acs.org>.

OM80001W